

Fabrication of Y-junction Metal Nanowires by AAO Template-assisted AC Electrodeposition

Huanan Duan¹, Zhenhai Xia² and Jianyu Liang^{1,*}

In this communication, we report a synthetic approach to fabricate Y-junction Co nanowires and Y-junction Cu nanowires by AC electrodeposition using a hierarchically designed anodized aluminum oxide template. Morphology study shows that diameters of the stems and branches of the Y-junction nanowires were about 40 nm and 20 nm respectively. Structural analysis indicates that Co nanowires had a mixture of face-center-cubic and hexagonal-close-packed structures, whereas Cu nanowires had a face-center-cubic structure with a <110> texture. The Y-junction Co nanowires exhibited a longitudinal coercivity of 1300 Oe and remnant magnetization of 56%, which was affected by the growth direction and microstructure. The present method can be extended to other metallic systems and thus provides a simple and efficient way to fabricate Y-junction metal nanowires.

Keywords: AAO template; Nanofabrication; AC electrodeposition; Y-junction metal nanowires; Magnetic property

Citation: Huanan Duan, Zhenhai Xia and Jianyu Liang, "Fabrication of Y-junction Metal Nanowires by AAO Template-assisted AC Electrodeposition", Nano-Micro Lett. 2, 290-295 (2010). [doi:10.3786/nml.v2i4.p290-295](https://doi.org/10.3786/nml.v2i4.p290-295)

Metal nanowires (NWs) have attracted vigorous research interests in recent years [1-11]. Among the numerous synthesis methods studied so far, fabrication inside rationally designed anodic aluminum oxide (AAO) templates has been proved to be an economic and versatile method to produce nanostructures with great efficiency and precision [2-4]. The AAO templates have many desirable characteristics such as a narrowly distributed pore size which can be tuned within a wide range, a well-developed fabrication process, easiness to remove, good mechanical and thermal stability, and chemical inertness. Since the pioneer work by T. M. Whitney [5], AAO template-assisted fabrication has achieved great success in the synthesis of linear metal nanowires [2-4,6-11]. Particularly, in applications such as nanoelectronics where nanowires with more complicated structure, such as Y-junction or branched NWs, are desirable, AAO template-assisted fabrication offers a simple and efficient method for the preparation of Y-junction metal NWs. Although in the past few years, a few reports were available on the synthesis of Y-junction carbon nanotubes [12,13] and metallic

Y-junction or branched nanowires by direct current (DC) electrodeposition [14-15], limited progress has been made on the synthesis of metallic Y-junction or branched nanowires by alternate current (AC) electrodeposition [20]. A typical synthesis process by DC electrodeposition is as following: firstly, the AAO templates are separated from the Al substrate; after the removal of the barrier layer, the templates are coated with a thin layer of noble metal to make an electrode; then target metal is deposited into the templates by DC electrodeposition. While AC electrodeposition has been proven to be a simple method to fabricate linear metal nanowires [6-11], using AC electrodeposition to fabricate metallic Y-junction NWs certainly demands more systematic exploration. Moreover, how the crystal structure and magnetic property of the synthesized Y-junction NWs are affected by the AC electrodeposition remains unclear.

In this paper, we report a generic synthetic approach to fabricate Y-junction metallic NWs including Co NWs and Cu NWs by AC electrodeposition using AAO templates with

¹Department of Mechanical Engineering, Worcester Polytechnic Institute, Worcester, MA 01609, USA

²Department of Mechanical Engineering, College of Engineering, The University of Akron, Akron, OH 44325, USA

*Corresponding author. E-mail: jjanyul@wpi.edu

well-controlled Y-junction channels. The morphology and structure of the NWs were characterized by scanning electron microscopy (SEM), transmission electron microscopy (TEM), selected area electron diffraction (SAED), and X-ray diffraction (XRD). The magnetic property of the Y-junction Co NWs was investigated by a conventional vibrating-sample magnetometer (VSM).

A schematic of the synthesis steps is shown in Fig. 1. The AAO templates were obtained by a well-established two-step anodization process [21-23]. Briefly, the first anodic oxidation of aluminum (99.999% pure, Electronic Space Products International) was carried out in a 0.3 M oxalic acid solution at 40 V and 10 °C for 16-20 h. The porous alumina layer formed during this first anodization step was completely dissolved by a mixture solution of 6% phosphoric acid and 1.8% chromic acid at 70 °C. The sample was then subjected to a second anodization where initially the anodization was performed under the same conditions as in the first anodization to produce the primary stem pores, and then the anodizing voltage was reduced by a factor of $1/\sqrt{2}$ to create the Y-branched pores. The as-prepared AAO templates were wet etched in 0.5% H_3PO_4 for half an hour to thin the barrier layer and widen the pores.

Cobalt nanowires were electrochemically deposited by AC electrolysis in this nanoporous template with Y-junction nanochannels using 14 V_{rms} at 100 Hz for 30 min in an electrolyte solution consisting of 240 g·l⁻¹ of $\text{CoSO}_4 \cdot 7\text{H}_2\text{O}$ (Alfa Aesar), 40 g·l⁻¹ of HBO_3 (Alfa Aesar), and 1 g·l⁻¹ of ascorbic acid (Alfa Aesar) [21-23]. Graphite was used as the counter electrode.

The synthesis of copper nanowires was adopted from G. A. Gelves's work [10, 11]. Electrodeposition of the Y-junction Cu NWs was carried out in an aqueous solution consisting of 0.50 M CuSO_4 (Alfa Aesar) and 0.285 M H_3BO_3 by applying a

continuous 200 Hz sine wave at 10 V_{rms} for 10 min between the anodized Al and the graphite counter electrode.

XRD patterns were recorded on a Rigaku Miniflex diffractometer using a $\text{Cu K}\alpha$ X-ray source (1.5405 Å). The structure and morphology were characterized by SEM using a JEOL JSM-7000F microscope and by TEM using a Phillips CM 12 operated at an accelerating voltage of 120 kV. TEM samples were prepared as follows: first the Y-junction NWs were liberated from the AAO template by dissolving the template in 2 M NaOH for 1 hour. After rinsing with DI water and dispersing the NWs in ethanol by sonication, a few drops of the solution were placed onto a carbon-coated Cu grid and dried in air. The magnetic property of the as-prepared Y-junction Co NWs was investigated using VSM with magnetic field in the range of -10,000 Oe to 10,000 Oe at room temperature.

Dimensions of the Y-junction AAO channels and the Y-junction metal NWs were analyzed using the image processing software of Image J [24]. Dimensions were measured at ten different locations on each of multiple SEM and TEM images and the average and standard deviation were reported.

The top-view SEM image (Fig. 2a) shows that nanopores within the AAO template form a highly ordered hexagonal pattern. The cross-section view SEM image (Fig. 2b) exhibits 5 micrometer long well-defined Y-junction channels within the AAO template. An arbitrary green line has been drawn to indicate the interface between the branches and the stems. Examination of Fig. 2b with Image J reveals that diameters of the stems and the branches of the Y-junction channels are 39.2 ± 4.2 nm and 19.6 ± 4.4 nm, respectively. It is notable that while the diameters of the branches are usually half that of the stems when the branches are formed at $1/\sqrt{2}$ of the voltage for the formation of the stems, the lengths of the stems and the branches of the

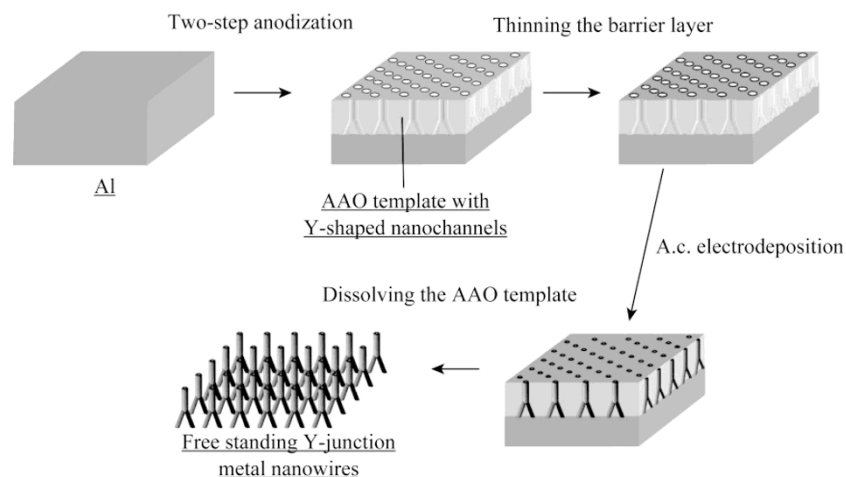


FIG. 1. Schematic of the process to synthesize Y-junction metal NWs.

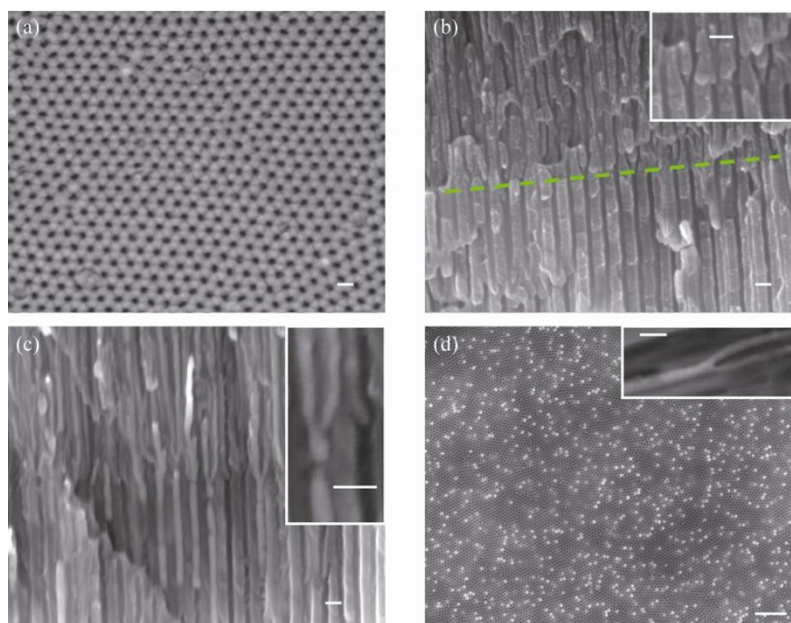


FIG. 2. SEM images of AAO templates with Y-junction nanochannels (a), (b), and after electrodeposition of Co (c) and Cu (d). Scale bar: 100 nm in all figures except the inset of (d); 1 μm in the inset of (d).

Y-junction channels can be independently adjusted by controlling the anodization duration for each segment.

Typical SEM images of the Y-junction Co NWs and Y-junction Cu NWs are shown in Fig. 2c and d. Clearly, NWs are parallel to each other and well contained in the Y-branched nanochannels. Statistical measurement by Image J shows that for Y-junction Co NWs, diameters of the stems and the branches are 39.3 ± 5.6 nm and 20.9 ± 4.8 nm, respectively; while for Y-junction Cu NWs, diameters of the stems and the branches are 40.3 ± 4.6 nm and 21.9 ± 4.2 nm, respectively. These diameters are in close agreement with the dimension of the Y-junction AAO nanochannels. Figure 2d also shows that 10 min deposition of Cu NWs can fill up some of 5 micrometer long AAO nanochannels.

XRD pattern for the Y-junction Co NWs embedded in the AAO template (Fig. 3(a)) shows that other than the Al peaks associated with the Al substrate (PDF card no. 04-0787), all peaks correspond to Co. Moreover, the Co NWs consist of a mixture of face-center-cubic (FCC) (PDF card no. 15-0806) and hexagonal-close-packed (HCP) (PDF card no. 05-0727) structures. The peak near 76° could be a combination of the diffraction from the (110) plane of the HCP structure and the (220) plane of the FCC structure, and the peak near 92.5° could be a combination of the diffraction from the (112) plane of the HCP structure and the (311) plane of the FCC structure. The coexistence of FCC and HCP structures has been observed in the electrodeposited straight Co NWs in previous studies using DC, AC, or pulsed deposition techniques [25-28]. It suggests a

complex growth mechanism because HCP and FCC Co NWs are generally believed to be obtained by two distinct mechanisms, namely, two-dimensional layer-by-layer growth and three-

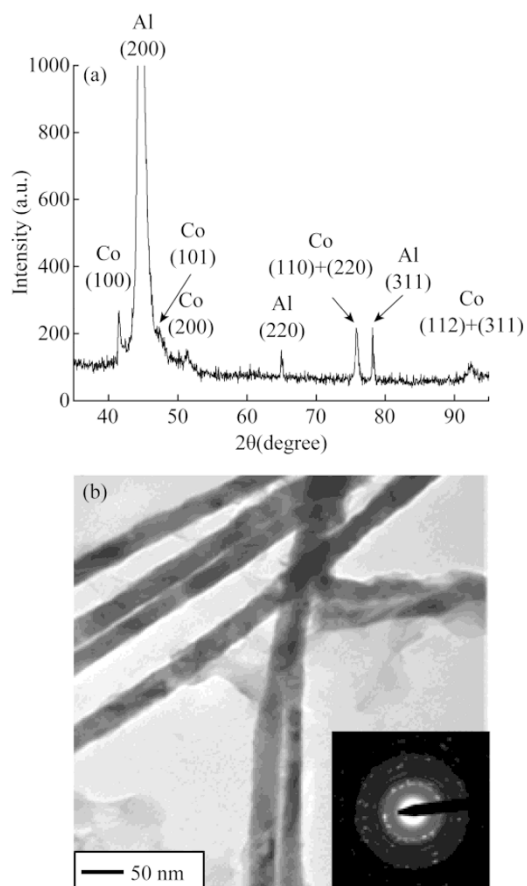


FIG. 3. (a) XRD pattern for the Y-junction Co NWs embedded in AAO template; (b) TEM of the Y-junction Co NWs. Inset: SAED patterns for (b).

dimensional nucleation/growth [29, 30]. The growth mechanism can be affected by the synthesis conditions such as pH value of the electrolyte [29], frequency of the power source [31], and the deposition potential [32].

Figure 3b shows a bright-field TEM image of Y-junction Co NWs. SAED was performed to investigate the crystalline structures of the Y-junction Co NWs. The broken ring SAED patterns suggest that the structures are polycrystalline in nature. The patterns are complicated due to the change of growth direction at the junction as well as the coexistence of HCP and FCC structures as shown in XRD results.

Due to the reduced dimension and the Y-shape, Y-junction Co NWs may possess unique magnetic properties. VSM was used to investigate the magnetic properties of the as-synthesized Y-junction Co NWs embedded in the AAO template. The hysteresis loops were recorded with the applied magnetic field parallel and perpendicular to the nanowire axis, respectively, at room temperature. As shown in Fig. 4, the coercivity, H_c , measured with the magnetic field perpendicular (transverse) to the wire axis is determined to be 486 Oe, much higher than 15 Oe, the value of straight single-crystal Co NWs reported [36]. In contrast, when the magnetic field is parallel (longitudinal) to the wire axis, H_c is determined to be 1300 Oe, around three times greater than the transverse value. The longitudinal H_c for straight Co NWs was reported in the range of 1100–2000 Oe [35, 36]. This enhanced longitudinal H_c suggests that the wire axis was the preferred overall magnetization direction. However, this enhancement was much less compared to straight Co NWs. Figure 4 also shows that the longitudinal remnant magnetization (M_r) equals to 56% of the saturated magnetization (M_s). The remnant magnetization is lower compared to that of the straight Co NWs, which was in the range of 67.8–80% [34–36]. We attribute this difference in the shape anisotropy and remnant

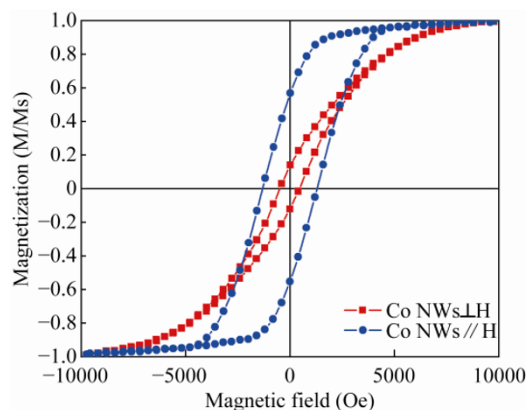


FIG. 4. Hysteresis behavior of the Y-junction Co nanowires with magnetic field H parallel and perpendicular to wire axis.

magnetization to the unique structure of the as-synthesized Y-junction Co NWs. For Y-junction Co NWs, the splitting of Co NWs and the change of growth direction near the Y junction affect the shape anisotropy. Moreover, the coexistence of HCP and FCC crystal structures by AC electrodeposition is another important factor because the coexistence may incur more complexity, inhomogeneity, and more domain structures compared to single-crystal Co NWs. It has been reported that for straight Co NWs with same diameters, the effective anisotropy along the nanowire axis of the FCC Co NW array is stronger than that of the HCP Co NW array [25].

The XRD pattern for the Y-junction Cu NWs (Fig. 5(a)) shows that the Cu NWs have a FCC structure (PDF card number: 04-0836) exhibiting a $\langle 110 \rangle$ texture, which is interesting because for bulk FCC structures the most energetically favorable texture is $\langle 111 \rangle$. One of the possible reason is that the adsorption of hydrogen may result in the stabilization of the (110) face during the electrodeposition of NWs in acidic solutions [33]. Moreover, at high overpotential the electrodeposited Cu NWs may undergo a thermodynamic to kinetic transition, producing [110] orientation [34].

Figure 5b depicts the TEM images of Y-junction Cu NWs. Analysis by Image J shows that the stems and branches of

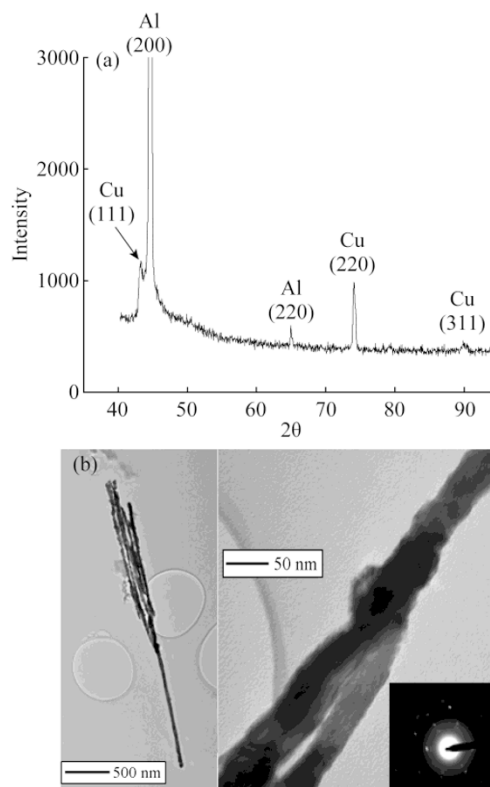


FIG. 5. (a) XRD pattern for the Y-junction Cu NWs embedded in AAO template; (b) TEM of the Y-junction Cu NWs. Inset: SAED patterns for (b) taken along the [111] zone axis perpendicular to the long axis of the NWs.

individual Y-junction Cu NWs have diameters of 42.8 ± 7.4 nm and 35.8 ± 5.3 nm, respectively. Similar analysis of TEM images of Y-junction Co NWs shows that diameters of the stems and branches are 42.2 nm \pm 4.0 nm and 28.1 nm \pm 4.2 nm, respectively. Clearly, the diameters of the stems and the branches of both metal NWs are considerably larger compared with the results estimated by SEM images. The dimensional increase may be due to the surface oxidation during the template removal or TEM sample preparation process [37]. The spotty diffraction rings in Fig. 5(b) (inset) show the polycrystalline nature of the Cu NWs.

In summary, by using a hierarchically designed AAO template, we fabricated Y-junction Co NWs and Y-junction Cu NWs by AC electrodeposition. Morphology study showed that well-defined Y-junctions were synthesized and dimensions of the NWs were defined by the template. Structure analysis indicated that the Co NWs were a mixture of FCC and HCP structures, and Cu NWs had FCC structure with a $\langle 110 \rangle$ texture. The coexistence of the FCC and HCP structures affected the coercivity and magnetization squareness of the Co NWs. The present method can be extended to other metallic systems and thus provide a simple and efficient way to fabricate Y-junction metal NWs.

This work is financially supported partially by a NSF award CMMI-0825990.

Received 7 November 2010; accepted 7 January 2011; published online 20 January 2011.

References

1. J. Wang, L. Y. Zhang, P. Liu, T. M. Lan, J. Zhang, L. M. Wei, E. S. Kong, C. H. Jiang and Y. F. Zhang, *Nano-Micro Lett.* 2, 134-138 (2010). [doi:10.5101/nml.v2i2.p134-138](https://doi.org/10.5101/nml.v2i2.p134-138)
2. H. Masuda, F. Hasegawa and S. Ono, *J. Electrochem. Soc.* 144, L127 (1997). [doi:10.1149/1.1837634](https://doi.org/10.1149/1.1837634)
3. A. P. Li, F. Muller, A. Birner, K. Nielsch and U. Gosele, *J. Appl. Phys.* 84, 6023 (1998). [doi:10.1063/1.368911](https://doi.org/10.1063/1.368911)
4. O. Jessensky, F. Muller and U. Gosele, *Appl. Phys. Lett.* 72, 1173 (1998). [doi:10.1063/1.121004](https://doi.org/10.1063/1.121004)
5. T. M. Whitney, J. S. Jiang, P. C. Searson and C. L. Chien, *Science* 261, 1316 (1993). [doi:10.1126/science.261.5126.1316](https://doi.org/10.1126/science.261.5126.1316)
6. A. J. Yin, J. Li, W. Jian, A. J. Bennett and J. M. Xu, *Appl. Phys. Lett.* 79, 1039 (2001). [doi:10.1063/1.1389765](https://doi.org/10.1063/1.1389765)
7. X. Y. Zhang, G. H. Wen, Y. F. Chan, R. K. Zheng, X. X. Zhang and N. Wang, *Appl. Phys. Lett.* 83, 3341 (2003). [doi:10.1063/1.1621459](https://doi.org/10.1063/1.1621459)
8. N. J. Gerein and J. A. Haber, *J. Phys. Chem. B* 109, 17372 (2005). [doi:10.1021/jp051320d](https://doi.org/10.1021/jp051320d)
9. R. L. Wang, S. L. Tang, B. Nie, X. L. Fei, Y. G. Shi and Y. W. Du, *Solid State Comm.* 142, 639 (2007). [doi:10.1016/j.ssc.2007.04.014](https://doi.org/10.1016/j.ssc.2007.04.014)
10. G. A. Gelves, B. Lin, U. Sundararaj and J. A. Haber, *Adv. Funct. Mater.* 16, 2423 (2006). [doi:10.1002/adfm.200600336](https://doi.org/10.1002/adfm.200600336)
11. G. A. Gelves, Z. T. Murakami, M. M. J. Krantz and J. A. Haber, *J. Mater. Chem.* 16, 3075 (2006). [doi:10.1039/b603442j](https://doi.org/10.1039/b603442j)
12. J. Li, C. Papadopoulos and J. Xu, *Nature* 402, 253 (1999). [doi:10.1038/46214](https://doi.org/10.1038/46214)
13. G. Meng, Y. J. Jung, A. Cao, R. Vajtai and P. M. Ajayan, *Proc. Natl. Acad. Sci.* 102, 7074 (2005). [doi:10.1073/pnas.0502098102](https://doi.org/10.1073/pnas.0502098102)
14. T. Gao, G. Meng, J. Zhang, S. Sun and L. Zhang, *Appl. Phys. A: Mater. Sci. Process.* 74, 403 (2002). [doi:10.1007/s003390101136](https://doi.org/10.1007/s003390101136)
15. J. Choi, G. Sauer, K. Nielsch, R. B. Wehrspohn and U. Gosele, *Chem. Mater.* 15, 776 (2003). [doi:10.1007/s003390101136](https://doi.org/10.1007/s003390101136)
16. Y. Tian, G. Meng, S. K. Biswas, P. M. Ajayan, S. Sun and L. Zhang, *Appl. Phys. Lett.* 85, 967 (2004). [doi:10.1063/1.1779956](https://doi.org/10.1063/1.1779956)
17. S. Mahima, R. Kannan, I. Komath, M. Aslam and V.K. Pillai, *Chem. Mater.* 20, 601 (2008). [doi:10.1021/cm702102b](https://doi.org/10.1021/cm702102b)
18. D. Li, C. Jiang, J. Jiang and J. G. Lu, *Chem. Mater.* 21, [doi:10.1021/cm8022242](https://doi.org/10.1021/cm8022242)
19. B. Chen, Q. Xu, X. Zhao, X. Zhu, M. Kong and G. Meng, *Adv. Funct. Mater.* 20, 3791 (2010). [doi:10.1002/adfm.201001190](https://doi.org/10.1002/adfm.201001190)
20. J. Zhang, C. S. Day and D. L. Carroll, *Chem. Comm.* 45, [doi:10.1039/b913917f](https://doi.org/10.1039/b913917f)
21. J. Liang, H. Chik, A. Yin and J. M. Xu, *J. Appl. Phys.* 91, 2544 (2002). [doi:10.1063/1.1433173](https://doi.org/10.1063/1.1433173)
22. J. Liang, H. Chik and J. M. Xu, *IEEE J. Sel. Top. Quantum Electron.* 8, 998 (2002). [doi:10.1109/JSTQE.2002.804238](https://doi.org/10.1109/JSTQE.2002.804238)
23. J. Li, C. Papadopoulos, J. M. Xu and M. Moskovits, *Appl. Phys. Lett.* 75, 367 (1999). [doi:10.1063/1.124377](https://doi.org/10.1063/1.124377)

24. <http://rsbweb.nih.gov/ij/>
25. F. Li, T. Wang, L. Ren and J. Sun, *J. Phys.: Condens. Matter.* 16, 8053 (2004). [doi:10.1088/0953-8984/16/45/027](https://doi.org/10.1088/0953-8984/16/45/027)
26. G. Tourillon, L. Pontonnier, J. P. Levy and V. Langlais, *Electrochem. Solid-State Lett.* 3, 20 (2000). [doi:10.1149/1.1390946](https://doi.org/10.1149/1.1390946)
27. G. J. Strijkers, J. H. J. Dalderop, M. A. A. Broeksteeg, H. J. M. Swagten and W. J. M. de Jonge, *J. Appl. Phys.* 86, 5141 (1999). [doi:10.1063/1.371490](https://doi.org/10.1063/1.371490)
28. N. R. Pradhan, H. Duan, J. Liang and G. S. Iannacchione, *Nanotech.* 19, 485712 (2008). [doi:10.1088/0957-4484/19/48/485712](https://doi.org/10.1088/0957-4484/19/48/485712)
29. H. Pan, H. Sun, C. Poh, Y. Feng and J. Lin, *Nanotech.* 16, 1559 (2005). [doi:10.1088/0957-4484/16/9/025](https://doi.org/10.1088/0957-4484/16/9/025)
30. M. Tian, J. Wang, J. Kurtz, T. E. Mallouk and M. H. Chan, *Nano Lett.* 3, 919 (2003). [doi:10.1021/nl034217d](https://doi.org/10.1021/nl034217d)
31. J. Zhang, G. A. Jones, T. H. Shen, S. E. Donnelly and G. Li, *J. Appl. Phys.* 101, 054310 (2007). [doi:10.1063/1.2464193](https://doi.org/10.1063/1.2464193)
32. X. W. Wang, G. T. Fei, P. Tong, X. J. Xu and L. D. Zhang, *J. Crystal Growth* 300, 421 (2007). [doi:10.1016/j.jcrysgro.2006.12.039](https://doi.org/10.1016/j.jcrysgro.2006.12.039)
33. J. A. Switzer, H. M. Kothari and E. W. Bohannon, *J. Phys. Chem. B* 106, 4027 (2002). [doi:10.1021/jp014638o](https://doi.org/10.1021/jp014638o)
34. H. Pan, B. Liu, J. Yi, C. Poh, S. Lim, J. Ding, Y. Feng, C. H. A. Huan and J. Lin, *J. Phys. Chem. B* 109, 3094 (2005). [doi:10.1021/jp0451997](https://doi.org/10.1021/jp0451997)
35. M. Darques, A. Encinas, L. Vila and L. Piraux, *J. Phys. D: Appl. Phys.* 37, 1411 (2004). [doi:10.1088/0022-3727/37/10/001](https://doi.org/10.1088/0022-3727/37/10/001)
36. Z. Liu, P. C. Chang, C. C. Chang, E. Galaktionov, G. Bergmann and J. G. Lu, *Adv. Funct. Mater.* 18, 1573 (2008). [doi:10.1002/adfm.200701010](https://doi.org/10.1002/adfm.200701010)
37. N. J. Gerein and J. A. Haber, *J. Phys. Chem. B* 109, 17372 (2005). [doi:10.1021/jp051320d](https://doi.org/10.1021/jp051320d)